Excluded volume effects in rotational-isomeric-state chains

D. Rigbyt and R. F. T. Stepto*
Department of Polymer Science and Technology, The University of Manchester Institute of Science and Technology, Sackville Street, PO Box 88, Manchester, M60 1QD, England, UK
(Received 21 April 1986; revised 14 July 1986; accepted 5 September 1986)

An algorithm improving the accuracy of Monte–Carlo calculations of the configurations of off-lattice polymer chains is described. It is used to investigate excluded-volume effects in rotational-isomeric-state polymethylene chains perturbed by Sutherland potentials and a particular Lennard–Jones potential. The importance of accounting properly for chain structure when determining expansion factors is clearly shown. The effective value of the segmental cluster integral is discussed in detail showing that it cannot be calculated directly from the potential function used but is strongly dependent on chain structure. Due to uneven chain expansion, i.e. the different perturbation of the various moments of the end-to-end distance distribution, θ-ranges rather than single θ-points are predicted at infinite chain length. The shortcomings of lattice models for chains are discussed, again emphasizing that chain structure must be included in calculations of chain expansion if meaningful interpretations of experimental expansion coefficients at different temperatures are to be achieved.

(Keywords: Monte–Carlo calculations; chain structure; perturbation; excluded volume; theta-point; cluster integral; chain expansion; chain contraction)

INTRODUCTION

The rotational-isomeric-state (RIS) description of the unperturbed dimensions of polymer chains[1] is widely accepted as satisfactory for interpreting mean-square end-to-end distances ($\langle r_0^2 \rangle$) and temperature coefficients ($d\ln\langle r_0^2\rangle/dT$) in terms of chain structures. In general, for reasonably flexible chains, two energy parameters describing energy differences between conformational states of sequences of four skeletal bonds are needed. Such RIS models account for the interdependence of contiguous pairs of rotational states $(t, g+, g-)$ of sequences of 3 skeletal bonds in that consecutive *gauche* states of opposite sign $(g\pm, g\mp)$ have an energy (E_ω) in addition to that of two independent *gauche* states, $2E_\sigma$. The values of $\langle r_0^2 \rangle$ from such interdependent RIS models may be denoted $\langle r_{0,\mathrm{int}}^2 \rangle$. If E_ω is neglected then 3-bond conformational states are independent and the mean-square end-to-end distance is denoted $\langle r_{0,\mathrm{ind}}^2 \rangle$.

The present paper takes the interdependent RIS model of Abe, Jernigan and Flory[2] (AJF) of the polymethylene (PM) chain to evaluate $\langle r_{0,\mathrm{int}}^2 \rangle$, as well as other moments of the end-to-end distribution ($\langle r_{0,\mathrm{int}}^q \rangle$) and investigates the effects of excluded volume on these dimensions in terms of uneven expansion and θ points. Expansion in terms of $\langle r_{0,\mathrm{ind}}^2 \rangle$ and the mean-square radius of gyration, $\langle s_{0,\mathrm{int}}^2 \rangle$, are also briefly considered. Solvent quality is mirrored by using several potential functions for effective segment–segment interactions. The potential functions allow chain expansion and contraction to occur so that comparisons can be made with lattice calculations and with predictions of analytical expressions for expansion factors. The calculations show the importance of accounting correctly for chain structure when correlating excluded volume with chain length and/or temperature.

Monte–Carlo calculations using Metropolis sampling have been used, and an algorithm is described which reduces rounding errors when sections of off-lattice chains are moved, as in the present work. The computational method has been used extensively in previous calculations of diffusion coefficients[3–7], comparisons of dimensions of lattice and off-lattice chains[8], chain folding[9], adsorption[10,11], comparative studies of linear and cyclic polymers[6,7,12–14], and particle scattering functions[14–16]. However, the algorithm has not been described previously.

CHAIN MODEL

Local interactions

Rather than use the terms short-range and long-range interactions, local and non-local interactions are preferred[8], as the real distinction between the two types is the chemical separation rather than the spatial separation of participating groups.

The AJF RIS model of the PM chain has geometric parameters[1,2], C–C bond length $(l) = 0.153$ nm, CCC bond-angle supplement $(\theta) = 68°$, and conformational angles $\phi_t = 0°$ and $\phi_{g\pm} = \pm 112.5°$. The energy parameters for local interactions are $E_\sigma = 1674$ J mol^{-1} (400 cal mol^{-1}) and $E_\omega = 6276$ J mol^{-1} (1500 cal mol^{-1}).

Non-local interactions

The representation of non-local interactions between pairs of segments in a polymer chain by simple potential functions necessarily introduces a certain arbitrariness.

* Proof to Dr R. F. T. Stepto, Störklingasse 44, CH-4125 Riehen, Switzerland.
† Present address: Department of Materials Science and Metallurgical Engineering, University of Cincinnati, Cincinnati, Ohio, 45221, USA.

0032-3861/87/030423-12$03.00

However, through the systematic variations of the numerical values of the parameters of the functions, comparative overall changes can be investigated. Also, it is important to remember that present theories of polymers in solution treat the solvent as a continuum. Potential energies of interaction are essentially effective energy differences derived from segment–segment, segment–solvent and solvent–solvent interactions according to the quasi-chemical equilibrium[10,11]. Thus, two segments at relative position vector $\boldsymbol{r}$ have an effective energy

$$E(\boldsymbol{r})=E_{22}(\boldsymbol{r})=2E_{12}(\boldsymbol{r})-2\Delta E_{12}(\boldsymbol{r})-E_{11}(\boldsymbol{r}) \quad (1)$$

where ΔE_{12} is the interchange energy of a solvent molecule (1) and a polymer segment (2) and is related to the Flory–Huggins interaction parameter χ (neglecting entropic contributions). Given the gross neglect of solvent structure, it is permissible to treat the polymer segments of non-polar chains as single, spherical entities and to use orientation-independent potential functions. In this case, scalar separations can be used in equation (1), and, for the PM chain, $-CH_2-$ units are taken as the segments.

The simplest function to use, which at least reflects dispersion–force laws, is the Sutherland potential function[11] having a hard-core repulsive potential and an r^{-6} dependence outside the hard-core. Thus,

$$E(r)=\infty, \quad r<r_c$$

and (2)

$$E(r)=cr^{-6}, \quad r\geqq r_c$$

where c and r_c are arbitrary constants. For a given polymer chain in solution, r_c may be taken as constant, at least to the same level of approximation that unperturbed dimensions (local interactions) are independent of solvent. Remembering equation (1), c may be positive or negative, i.e.

$$E(r)=cr^{-6}=(2c_{12}-2\Delta c_{12}-c_{11})r^{-6} \quad (3)$$

where $E_{12}(r)=c_{12}r^{-6}$, etc. As c increases the quality of solvent improves. At some negative value of c, θ behaviour (unperturbed dimensions) will occur. When $c=0$, the chain is one of spherical, hard-core segments. Although, for $c=0$, the energy per non-local interaction will be independent of temperature, the excluded volume of the chain will still vary with temperature because the unperturbed dimensions (populations of t and g states) so vary and give different numbers of segment overlaps. Such a temperature dependence of excluded volume does not arise if idealised, random-flight chains are used as the unperturbed basis. When $c>0$, $E(r)$ decreases continuously as a function of r, for $r\geqq r_c$. The majority of the calculations in the present paper have used Sutherland potential functions.

The Lennard–Jones (L–J) potential function has often been used in Monte–Carlo calculations. However, the advantages gained in the context of polymer solutions are hard to see. One cannot easily keep the repulsive core constant and systematically vary the attractive potential. In this potential function

$$E(r)=4\varepsilon^*\left(\left(\frac{r^*}{r}\right)^{12}-\left(\frac{r^*}{r}\right)^{6}\right) \quad (4)$$

$E=0$ when $r=r^*$, and $E=-\varepsilon^*$ defines the minimum of the potential well, situated at $(r^*/r)=2^{1/6}$. In order to compare the behaviour of the Sutherland and L–J functions, one particular L–J function was used in the present investigation, namely, that with 'consistent parameters' (CP). These parameters were defined so that the *local* (t,g) energies of $-CH_2-$ groups at their various separations were consistent with the non-local energies from the L–J potential. Consider the t and g states of a three-bond (butane) sequence in the chain; denote their energies by E_1 and E_2 and their end-to-end separations by r_1 and r_2, respectively. Similarly, let the $g\pm g\pm$ and $g\pm g\mp$ states of a four-bond (pentane) sequence have energies E_3 and E_4 and end-to-end separations r_3 and r_4. In order to make local and non-local interactions consistent, one puts $E_2-E_1=E_\sigma$ and $E_4-E_3=E_\omega$, to give the two equations

$$E_\sigma=4\varepsilon^*\left(\left(\frac{r^*}{r_2}\right)^{12}-\left(\frac{r^*}{r_1}\right)^{12}-\left(\frac{r^*}{r_2}\right)^{6}+\left(\frac{r^*}{r_1}\right)^{6}\right) \quad (5)$$

and

$$E_\omega=4\varepsilon^*\left(\left(\frac{r^*}{r_4}\right)^{12}-\left(\frac{r^*}{r_3}\right)^{12}-\left(\frac{r^*}{r_4}\right)^{6}+\left(\frac{r^*}{r_3}\right)^{6}\right) \quad (6)$$

Equations (5) and (6) can be solved for r^* and ε^*. The values so obtained were $r^*=0.3264$ nm and $\varepsilon^*=603.2\,\mathrm{J\,mol^{-1}}$. By using these consistent parameters, $-CH_2/-CH_2-$ interactions follow a single law independent of the relative chemical positions in the chain of the interacting groups. By way of contrast, Lal and Spencer[17] (LS) used values of r^* and ε^* derived from data on bulk polyethylene. r^* was estimated at 0.419 nm from the $-CH_2-\ldots-CH_2-$ separation in solid polyethylene at 0K, and ε^* as $318.0\,\mathrm{J\,mol^{-1}}$ ($76.0\,\mathrm{cal\,mol^{-1}}$) from the heat of sublimation. This potential gives values of $95.8\,\mathrm{kJ\,mol^{-1}}$ and $36.7\,\mathrm{kJ\,mol^{-1}}$ for E_σ and E_ω, respectively. Remembering that the values of $1.674\,\mathrm{kJ\,mol^{-1}}$ and $6.276\,\mathrm{kJ\,mol^{-1}}$ are those of the more normally used AJF model of the PM chain, the L–J/LS potential gives large excluded volume effects.

Parameters of the Sutherland potential functions used

For all the potentials, r_c was set at 0.27 nm. This value had been used previously[8] as it is equal to the distance between the 'prow' and 'stern' $-CH_2-$ groups in the boat form of cyclohexane.

The values of c used were chosen partly in relation to characteristics of the L–J/CP function. One characteristic used was ε^* and the other was the binary cluster integral, β, usually taken as the chain-length-independent parameter for describing excluded-volume effects. The value to be calculated for a given potential function is

$$\beta_{calc}=\int_0^\infty (1-\exp(E(r)/RT))4\pi r^2 dr. \quad (7)$$

It assumes that the separation of a pair of segments can vary from 0 to ∞. Its effective values (β_{eff}) for various chain lengths will be discussed later. For accuracy of numerical evaluation of β_{calc} for the Sutherland potential (equation (2)) using standard integration routines, equation (7) was transformed to

$$\beta_{calc} = 4\pi r_c^3/3 + \int_0^1 (4\pi r_c^3/x^4)(1-\exp(h(x))dx, \quad (8)$$

where $x = r_c/r$ and $h(x) = -(c/RT)(x/r_c)^6$.

The values of c of the Sutherland potential functions employed are given in *Table 1*, and the variations of β_{calc} with temperature for these and the L–J/CP and the L–J/LS potentials are shown in *Figure 1*. Apart from the potentials chosen for comparison with the L–J/CP function, those with equal intervals in $E(r_c)$ were used as well as that with $c=0$. More functions with negative values of c were employed so that θ-behaviour could be investigated.

COMPUTATIONAL METHODS

Complete enumeration

The general method used has been described previously[9,18] and only the main points are given here. The complete enumeration of the energies and required properties of all the 3^{x-3} configurations of a chain of x segments was possible for $x \leqslant 16$ using the CDC 7600 computer at the University of Manchester.

If configuration j has energy E_j, which is the sum of its local and non-local energies, and property p_j, then the required configurational average of p is

$$\langle p \rangle = \sum_j p_j \exp(-E_j/RT) / \sum_j \exp(-E_j/RT), \quad (9)$$

where, for the present work, p is equal to r^q, $q = 1,2,\ldots 10$, and to s^2. Using complete enumeration, the denominator in equation (9) is the configurational partition function of the chain model used. With the inclusion of non-local interactions, the coordinates of all chain segments are required to give distances r_{ik}, allowing $E(r_{ik})$ to be found from equations (2) or (4) for all distinct pairs of segments, with $k-i \geqslant 5$. The total energy of the all-*trans* chain $(E_{l,trans} + E_{n-l,trans})$ is taken as zero. The local energy, $E_{l,trans}$, is already defined as zero. Hence, the non-local energy, $E_{n-l,trans}$, is evaluated first and subtracted from the non-local energies of all subsequent configurations. Calculations with unperturbed chains do not require knowledge of the coordinates of all segments, except as required by the particular property being considered, e.g. $\sum_{i<k} r_{ik}^2$ for $\langle s_0^2 \rangle$. Only knowledge of the set of conformational angles for configuration j, $\{\phi\}_j$, and the resulting $E_{l,j}$ is required.

The vector connecting segment i to segment k $(i<k)$ may be written

$$\boldsymbol{r}_{ik} = \boldsymbol{l}_{i+1} + \underline{T}_{i+1}\boldsymbol{l}_{i+2} + \underline{T}_{i+1}\underline{T}_{i+2}\boldsymbol{l}_{i+3} + \cdots \underline{T}_{i+1}\cdots\underline{T}_{k-1}\boldsymbol{l}_k, \quad (10)$$

where, according to the usual notation[1], for a chain of n bonds, the segments are numbered 0 to n, $\boldsymbol{l}_m$ is the bond vector ending at segment m, and $\underline{T}_m$ is the transformation matrix defining rotation about m to bring the coordinate system of bond $m+1$ parallel to that of bond m. For the PM chain, $\boldsymbol{l}_i = [l,0,0]^T$, and

$$\underline{T}_i = \begin{bmatrix} \cos\theta & \sin\theta & 0 \\ \sin\theta.\cos\phi_i & -\cos\theta.\cos\phi_i & \sin\phi_i \\ \sin\theta.\sin\phi_i & -\cos\theta.\sin\phi_i & -\cos\phi_i \end{bmatrix} \quad (11)$$

Complete enumeration merely requires the generation of sequences of $n-2\phi$'s which are coded as integers according to the convention $\phi_i = 1, 2, 3$, respectively for t, $g+$ and $g-$. The initial, all-*trans* configuration is therefore a series of 1's. The energy of this chain is calculated and its properties evaluated. Subsequent configurations are then generated by changing individual ϕ's in a cyclic manner, starting with ϕ_{n-1}, and the sums in

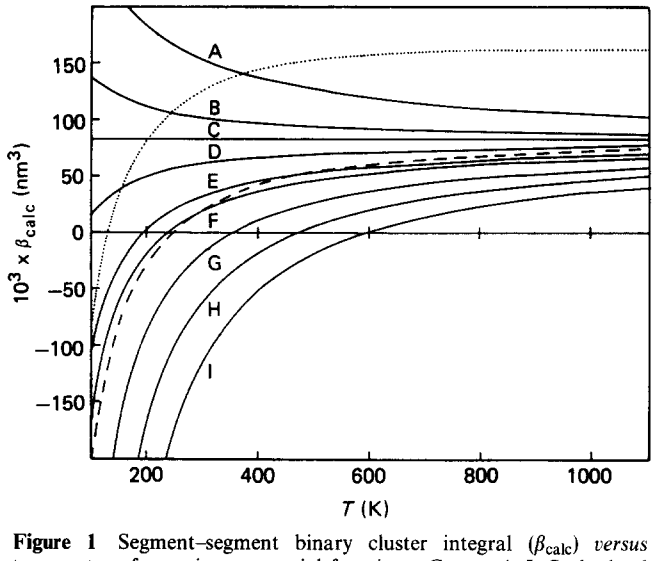

Figure 1 Segment–segment binary cluster integral (β_{calc}) *versus* temperature for various potential functions. Curves A–I, Sutherland potentials with values of c given in *Table 1*. (– – –) Lennard-Jones consistent parameter (L–J/CP) potential. (· · · · ·) Lennard-Jones, Lal and Spencer (L–J/LS) potential[17]

Table 1 Values of the parameter c used in calculations with the Sutherland potential function, equation (2). $E(r_c)$ – energy at $r = r_c$, where $r_c = 0.27$ nm. The letters to the left correspond to the curves in *Figure 1*

	$E(r_c)$ J mol^{-1} (cal mol^{-1})	c (J nm^6 mol^{-1})	Comments
1	2510 (600)	0.9726	
2	603.2 (144.16)	0.2337	
3	0 (0)	0	
4	−603.2 (−144.16)	−0.2337	same minimum ($-\varepsilon^*$) as L–J/CP
5	−1351 (−323)	−0.5236	same β_{calc} as L–J/CP at 500 K
6	−1678 (−401)	−0.6500	same β_{calc} as L–J/CP at 298.2 K
7	−2510 (−600)	−0.9726	
8	−3347 (−800)	−1.2930	
9	−4184 (−1000)	−1.6210	

equation (9) are built up, term-by-term, as each configuration is generated.

Metropolis sampling

In the Metropolis procedure[10,11] the configurations of randomly chosen sections of the chain are changed. A new configuration is accepted or rejected according to criteria which, in the limit of an infinite sample, result in configurations being generated with frequencies proportional to their Boltzmann factors, $\exp(-(E_l+E_{n-l})/RT)$. Thus, equation (9) is replaced by the simple average

$$\langle p\rangle = \sum_{j=1}^{N} p_j/N \tag{12}$$

for a sample of N configurations. The method gives more rapid convergence, to better than 1% in $\langle r^2\rangle$, than random sampling. As only part of the chain is altered between configurations, the method has proved particularly suitable for cyclic chains[6,7,12-14], and for calculations involving a molecule moving in an external reference frame, e.g. for adsorption onto a surface[10,11,19] or centre-of-mass diffusion[20].

The length of section of chain over which contiguous conformational angles are changed in a Metropolis move is arbitrary. Tests in the present work on PM chains showed that the fastest convergence was usually obtained when two adjacent ϕ's were changed. However, up to four contiguous conformations per move were sometimes used. Care must be taken that the particular end of the molecule which moves in the external coordinates is chosen randomly. In addition, rounding errors, which result from the numerous matrix multiplications required to determine coordinate positions must not be allowed to become significant.

Metropolis moves: Internal coordinates

The segments are still numbered 0 to n, with 0 denoting the leading end of a chain and n the trailing end. A sequence of v bonds is chosen randomly to undergo conformational change, with the proviso that less than v bonds can be moved if a chain end is encountered. In this way, each bond has an equal probability of undergoing a conformational change. The change of conformations of a sequence of bonds within a chain causes the segments in that sequence *and* one of the chain ends to move in external space. The particular end to move is chosen randomly. If the trailing end is moved, then equation (10) can be used to generate coordinates $\boldsymbol{r}_{ik}$ $(k>i)$. The conventional right-handed (r.h.) internal, local coordinate systems for the bond vectors, consistent with equation (11), is used[1], with positive directions going from 0 to n, as shown in *Figure 2a*. For movement of the leading end, a 'reverse' set of r.h. local, internal coordinates may conveniently be defined, as in *Figure 2b*. The bond vector from segment i *to* $i-1$ is denoted $\boldsymbol{l}'_{i-1}$. The coordinate system centred on segment i has X'_{i-1} lying along $\boldsymbol{l}'_{i-1}$, Y'_{i-1} giving a positive projection on the preceding bond (X'_i), and Z'_i completing a r.h. system. θ'_{i-1} and ϕ'_{i-1} are as shown in *Figure 2b* with ϕ'_{i-1} r.h. positive. The vector $\boldsymbol{r}'_{ik}$ is now given by the equation

$$\boldsymbol{r}'_{ik} = \boldsymbol{l}'_{i-1} + \underline{T}'_{i-1}\boldsymbol{l}'_{i-2} + \ldots + \underline{T}'_{i-1}\underline{T}'_{i-2}\cdots\underline{T}'_{k+1}\boldsymbol{l}'_k, \tag{13}$$

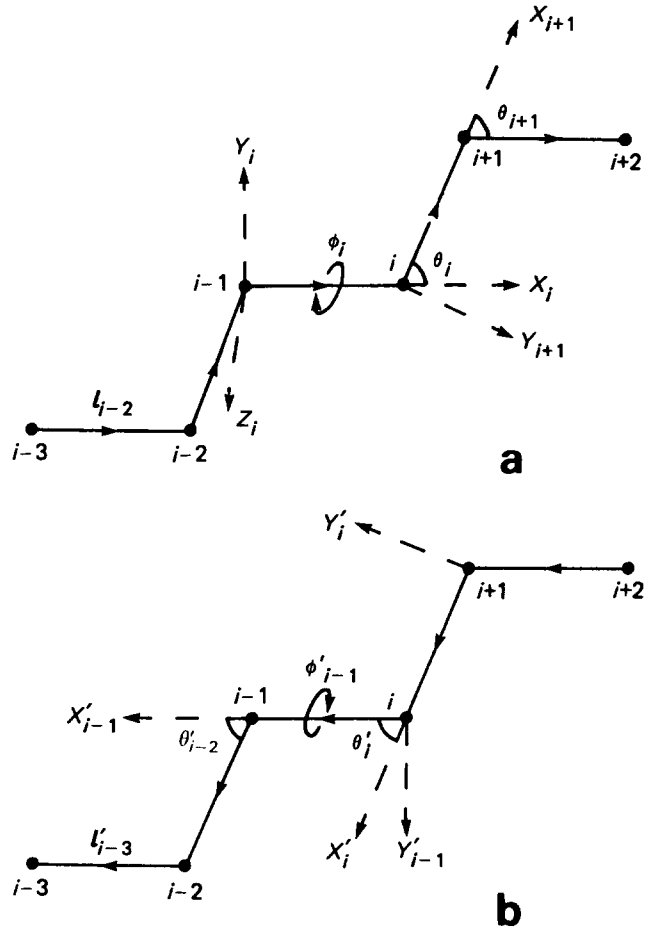

Figure 2 Definition of right-handed, internal local coordinate systems for the movement of (a) trailing and (b) leading chain ends

where $\underline{T}'_i$ is the matrix obtained from equation (11) by replacing $\underline{T}_i$, θ_i and ϕ_i respectively by $\underline{T}'_i$, θ'_i, and ϕ'_i. The chain parameters of the reverse and forward sets are easily related as

$$\theta'_i = \theta_i, \tag{14}$$

$$\phi'_{i-1} = \phi_i, \tag{15}$$

and

$$l'_{i-1} = l_i. \tag{16}$$

In addition, when considering a chain in which all valence angles are the same,

$$\underline{T}'_{i-1} = \underline{T}_i. \tag{17}$$

Metropolis moves: External coordinates

The local coordinates of segment j may be transformed to external coordinates using the general relationship

$$\boldsymbol{R}_j = \boldsymbol{a}_j + \underline{P}\boldsymbol{r}_j \tag{18}$$

$\boldsymbol{R}_j$ and $\boldsymbol{r}_j$ are, respectively, the position vectors in the external and internal systems, $\boldsymbol{a}_j$ is the shift vector (translation) connecting the origins of the two systems, and $\underline{P}$ is the rotation matrix between the two. For a given move of v segments in internal coordinates, $\boldsymbol{a}_j$ and $\underline{P}$ need to be evaluated for all the segments which move in the

external frame. $\underline{\underline{P}}$ may be evaluated provided that during a move in the external coordinates of any three contiguous (reference) segments are fixed. To decide which remain fixed, it is first decided randomly whether the leading or trailing end is to be moved. Then a segment, k, is chosen at random to be the origin of the internal system. For a move of the trailing end, k is chosen from the set of integers $\{0,1\ldots,n-3\}$, whilst, for a move of the leading end, the corresponding set is $\{3,4,\ldots,n\}$. With k chosen, the reference coordinates to be used for the determination of $\underline{\underline{P}}^k$ may be taken as those of segments k, $k+1$ and $k+2$ if the trailing end is moved, and those of k, $k-1$ and $k-2$ if the leading end is moved. Both these cases may be denoted k, $k+t$, and $k+2t$, where $t=1$ and -1, respectively, for moves of the trailing and leading ends. The respective conformation angles to be changed are $\phi_{k+2},\ldots,\phi_{k+1+v}$ and $\phi'_{k-2},\ldots,\phi'_{k-1-v}$. Thus, the external coordinates of segments $0,1,\ldots,k+2$ remain fixed for moves of the trailing end, whilst those of segments $n,n-1,\ldots,k-2$ remain fixed for moves of the leading end (c.f. *Figures 2a* and *2b* with k substituted for i).

All chain configurational energies are expressed relative to that of the all-*trans* chain. Hence, it is convenient to generate this configuration first by locating segment 0 at the origin of the external system (i.e. $\boldsymbol{a}=[0,0,0]^T$) and setting $\underline{\underline{P}}^0=\text{diag}\,[1,1,1]^T$. In this way, the internal coordinate system defined by the first two bonds coincides with the external system. Construction of the remainder of the chain in the direction of the trailing end then follows the method used for exact enumeration. The non-local interaction energies are then calculated.

The initial configuration of the Metropolis sequence is then generated according to the previous code, 1 for ϕ_t, 2 for ϕ_{g^+} and 3 for ϕ_{g^-}. Segment 0 is left at the origin of the external coordinate system, but the rotation matrix P^0 is chosen randomly through three Euler angles, α, β and γ, relating the internal and external systems. $\underline{\underline{P}}$ is generally the matrix of direction cosines between the axes, given by the following standard relationships[21]

$$\begin{aligned}
P_{xx}&=\cos\alpha\cos\beta\cos\gamma-\sin\alpha\sin\gamma\\
P_{xy}&=\sin\alpha\cos\beta\cos\gamma+\cos\alpha\sin\gamma\\
P_{xz}&=-\sin\beta\cos\gamma\\
P_{yx}&=-\cos\alpha\cos\beta\sin\gamma-\sin\alpha\cos\gamma\\
P_{yy}&=-\sin\alpha\cos\beta\sin\gamma+\cos\alpha\cos\gamma\\
P_{yz}&=\sin\beta\sin\gamma\\
P_{zx}&=\cos\alpha\sin\beta\\
P_{zy}&=\sin\alpha\sin\beta\\
P_{zz}&=\cos\beta
\end{aligned}\qquad(19)$$

As stated, subsequent configurations are generated by choosing randomly segment k, keeping segments k, $k+t$, and $k+2t$ fixed, and changing randomly the next v conformational angles, causing the trailing or leading ends of the chain adjacent to $k+2t$ to move in external space. Use of equation (10) in equation (18) gives for the trailing end ($j>k$)

$$\boldsymbol{R}_j=\boldsymbol{a}_k+\underline{\underline{P}}^k\boldsymbol{l}_{k+1}+\underline{\underline{P}}^k\underline{\underline{C}}_{k+1}\boldsymbol{l}_{k+2}+\cdots+\underline{\underline{P}}^k\underline{\underline{C}}_{k+1}\underline{\underline{T}}_{k+2}\cdots\underline{\underline{T}}_{j-1}\boldsymbol{l}_j\qquad(20)$$

and equation (13) in equation (18) gives for the leading end ($j<k$)

$$\boldsymbol{R}_j=\boldsymbol{a}_k+\underline{\underline{P}}^k\boldsymbol{l}'_{k-1}\underline{\underline{P}}^k\underline{\underline{C}}'_{k-1}\boldsymbol{l}'_{k-2}+\cdots+\underline{\underline{P}}^k\underline{\underline{C}}'_{k-1}\underline{\underline{T}}'_{k-2}\cdots\underline{\underline{T}}'_{j+1}\boldsymbol{l}'_j\qquad(21)$$

The shift vector

$$\boldsymbol{a}_k=[X_k,Y_k,Z_k]^T\qquad(22)$$

is known from the previous configuration. The matrices $\underline{\underline{C}}_{k+1}$ and $\underline{\underline{C}}'_{k-1}$, are those obtained from $\underline{\underline{T}}_i$ (equation (11)) but with $\phi_{k+1}=\phi'_{k-1}=0$. This substitution follows from the fixing of segments k, $k+t$ and $k+2t$ in the X,Y plane of the external coordinate system. The use of equations (20) and (21) means that unnecessary matrix multiplications are avoided. Products such as $\underline{\underline{P}}^k\underline{\underline{C}}_{k+1}\underline{\underline{T}}_{k+2}$ are stored and only one further multiplication needs be performed for each bond added.

The matrix $\underline{\underline{P}}^k$ now needs to be determined. To do this equation (18) is used to define differences between the external coordinates of segments k to $k+2t$, giving, in terms of components,

$$\begin{aligned}
X_{k+t}-X_k&=P_{xx}(x_{k+t}-x_k)+P_{xy}(y_{k+t}-y_k)+P_{xz}(z_{k+t}-z_k)\\
X_{k+2t}-X_k&=P_{xx}(x_{k+2t}-x_k)+P_{xy}(y_{k+2t}-y_k)\\
&\quad+P_{xz}(z_{k+2t}-z_k),
\end{aligned}\qquad(23)$$

with corresponding pairs of equations for $Y_{k+t}-Y_k$ and $Y_{k+2t}-Y_k$, and $Z_{k+t}-Z_k$ and $Z_{k+2t}-Z_k$. The internal (x,y,z) coordinates of segments k, $k+t$ and $k+2t$ are, respectively, (0,0,0), $(l^*_{k+t},0,0)$ and $(l^*_{k+t}+l^*_{k+2t}\cos\theta^*_{k+t}$, $l^*_{k+2t}\sin\theta^*_{k+t},0)$, where the l^* are the scalar lengths of the corresponding vectors $\boldsymbol{l}$ and $\boldsymbol{l}'$, and θ^* is the supplement of the appropriate valence angle. Elimination of the differences between internal coordinates in equation (23) then gives for six elements of $\underline{\underline{P}}^k$

$$\begin{aligned}
P_{xx}&=(X_{k+t}-X_k)/l^*_{k+t}\\
P_{yx}&=(Y_{k+t}-Y_k)/l^*_{k+t}\\
P_{zx}&=(Z_{k+t}-Z_k)/l^*_{k+t}
\end{aligned}\qquad(24)$$

$$\begin{aligned}
P_{xy}&=(X_{k+2t}-X_{k+t}-P^k_{xx}l^*_{k+2t}\cos\theta^*_{k+t})/l^*_{k+2t}\sin\theta^*_{k+t}\\
P_{yy}&=(Y_{k+2t}-Y_{k+t}-P^k_{yx}l^*_{k+2t}\cos\theta^*_{k+t})/l^*_{k+2t}\sin\theta^*_{k+t}\\
P_{zy}&=(Z_{k+2t}-Z_{k+t}-P^k_{zx}l^*_{k+2t}\cos\theta^*_{k+t})/l^*_{k+2t}\sin\theta^*_{k+t}
\end{aligned}\qquad(25)$$

The remaining three components can then be found using the orthogonality relationships for the direction cosines of a r.h. system, namely[22]

$$\begin{aligned}
P_{xz}&=P_{yx}.P_{zy}-P_{zx}.P_{yy}\\
P_{yz}&=P_{zx}.P_{xy}-P_{xx}P_{zy}\\
P_{zz}&=P_{xx}.P_{yy}-P_{yx}.P_{xy}.
\end{aligned}\qquad(26)$$

In order to apply this scheme successfully in practice, it is necessary to appreciate that, due to rounding errors arising from successive multiplications, the bond lengths l^*_{k+t} and l^*_{k+2t}, and the valence angle supplement θ^*_{k+t} will not be numerically equal to the values used when the chain was originally constructed. To obtain an accurate evaluation of $\underline{\underline{P}}$ it is necessary to calculate these quantities

directly from the machine-stored, external coordinates of the appropriate segments. Thus,

$$l^*_{k+t}=((X_{k+t}-X_k)^2+(Y_{k+t}-Y_k)^2+(Z_{k+t}-Z_k)^2)^{1/2}$$

and

$$l^*_{k+2t}=((X_{k+2t}-X_k)^2+(Y_{k+2t}-Y_k)^2+(Z_{k+2t}-Z_k)^2)^{1/2} \quad (27)$$

Also,

$$\begin{aligned}\cos\theta^*_{k+t}&=(\underline{l}^*_{k+t}.\underline{l}^*_{k+2t})/l^*_{k+t}l^*_{k+2t}\\&=((X_{k+t}-X_k)(X_{k+2t}-X_{k+t})+(Y_{k+t}-Y_k)\\&\quad\times(Y_{k+2t}-Y_{k+t})+(Z_{k+t}-Z_k)\\&\quad\times(Z_{k+2t}-Z_{k+t}))/l^*_{k+t}l^*_{k+2t}.\end{aligned} \quad (28)$$

Estimation of rounding errors in moves in external coordinates

Calculations were performed in which N different configurations were generated by changing sequences of 1 and 4 contiguous conformational angles. The Metropolis criteria were not applied as only the build-up of rounding errors was investigated. The mean-square error in l, for example, was calculated as

$$\langle\Delta l^2\rangle=\frac{1}{N}\sum_{j=1}^{N}\left\{\frac{1}{n}\sum_{i=1}^{n}(l_i-l_i^*)^2\right\}_j, \quad (29)$$

where N is the number of configurations generated, n the number of bonds in the chain, l_i the true bond length and l_i^* the bond length from machine-stored coordinates of segments. $\langle\Delta l^2\rangle^{1/2}/l$ at worse is increased to about 5×10^{-12} (3 significant figures on the computer used) after 10^5 configurations. This value may be compared with that of 10^{-9} to 10^{-7} (6–8 significant figures) after 10^3 to 10^4 configurations when actual values of l_i, $\cos\theta_i$ and $\sin\theta_i$ were used to calculate $\underline{P}$ from equations (24) to (26). Errors in $\cos\theta$ and $\cos\phi$ were also investigated and similar reductions were found.

RESULTS AND DISCUSSION

Variation of $\langle r^2\rangle/n$ *with* n *and* T

Figure 3 shows the commonly used characteristic ratio $\langle r^2\rangle/n$ as a function of n at various temperatures. The curves illustrate the general variation of this quantity in the presence of an attractive potential, the L-J/CP potential. Also shown are $\langle r^2_{0,\mathrm{int}}\rangle/n$ and $\langle r^2_{0,\mathrm{ind}}\rangle/n$ which may be used as different bases to calculate expansion factors.

The $\langle r^2\rangle/n$ curves are seen to pass through maxima which become sharper and occur at shorter chain lengths as temperature decreases. Such behaviour reflects the fact that beyond a certain chain length ($n=17$ with this particular potential) the all-*trans* chain is no longer the lowest-energy form of the isolated chain, and, as T decreases, compact configurations of low energy dominate the average dimensions. The details of such configurations have been discussed previously in the context of chain folding[9].

Because the L-J/CP potential has been used, the ratios of $\langle r^2\rangle/n$ to $\langle r^2_{0,\mathrm{int}}\rangle/n$ and $\langle r^2_{0,\mathrm{ind}}\rangle/n$ define expansion coefficients (α^2_r) on a consistent basis but relative to different unperturbed dimensions, giving widely different values of α^2_r. The dotted curve at $T=\infty$, with all

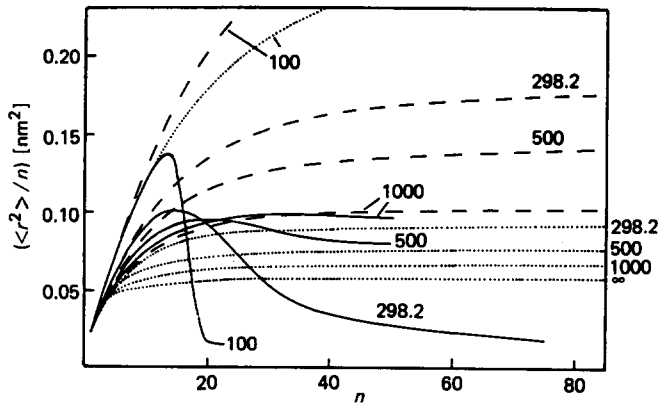

Figure 3 Characteristic ratios $\langle r^2\rangle/n$ *versus* number of bonds (n) for AJF RIS model PM chains. (———) Interdependent RIS model with non-local interactions given by the L-J/CP potential. (– – –) Unperturbed interdependent RIS model ($\langle r^2_{0,\mathrm{int}}\rangle/n$). ····· Unperturbed independent RIS model ($\langle r^2_{0,\mathrm{ind}}\rangle/n$). Values of T (K) given with curves

conformational angles of equal statistical weight, gives the unperturbed dimensions of freely-rotating chains ($\langle r^2_{0,\mathrm{f}}\rangle$), similar to those of random-choice tetrahedral-lattice calculations (except that $\theta=68°$ and not $\cos^{-1}(\frac{1}{3})$). The other dotted curves, with independent rotational states, give unperturbed dimensions ($\langle r^2_{0,\mathrm{ind}}\rangle$) similar to those used by Lal and collaborators[10,17,23]. The dashed curves give unperturbed dimensions with interdependent rotational states ($\langle r^2_{0,\mathrm{int}}\rangle$) which relate more closely to the actual behaviour of unperturbed PM chains. The differences in magnitudes of the values of α^2_r which would result, from using the three different unperturbed dimensions, $\langle r^2_{0,\mathrm{f}}\rangle$, $\langle r^2_{0,\mathrm{ind}}\rangle$ and $\langle r^2_{0,\mathrm{int}}\rangle$, are immediately apparent from *Figure 1*. In addition, and more importantly, the three sets of expansion factors will not scale one to the other because the temperature coefficients of the unperturbed chains are different. $\langle r^2_{0,\mathrm{f}}\rangle$ is independent of temperature, and the ratio $\langle r^2_{0,\mathrm{int}}\rangle/\langle r^2_{0,\mathrm{ind}}\rangle$ increases as temperature decreases. The lack of scaling emphasizes the importance of using the correct unperturbed dimensions of actual chains when attempting to interpret their excluded volume behaviour at various temperatures.

Figure 4 shows $\langle r^2_{0,\mathrm{int}}\rangle/n$ and $\langle r^2\rangle/n$ for two Sutherland potentials with $c=0$ and $c=-0.65$ J nm^6 mol^{-1}. Marked chain contraction is apparent at 298.2 K for the latter potential, but to a lesser extent than for the L-J/CP potential. This relative behaviour illustrates effects of the shape of the potential function, as both functions have the same value of β_{calc} (see *Table 1*). The weaker, overall attraction of the Sutherland potential is also indicated by the facts that it gives only a shallow maximum at 500 K and no indication of a maximum at 1000 K for chains up to 100 bonds. At sufficiently high temperatures, for any potential for which $E(r)\to0$ as $r\to\infty$, it is only the interactions at small r_{ij} (repulsive) which will perturb the dimensions and cause expansion rather than contraction (see later).

The hard-core potential ($c=0$) has often been used in lattice calculations of excluded volume in the guise of nearest-neighbour interaction. It is apparent that it cannot be used to describe chain contraction. Also, although the potential itself has a cluster integral independent of temperature, the chain expansion predicted on the basis of $\langle r^2_{0,\mathrm{int}}\rangle$ increases with

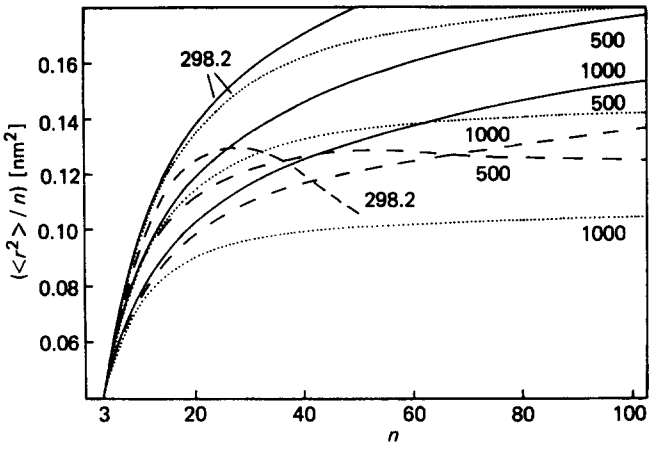

Figure 4 $\langle r^2\rangle/n$ *versus* n for AJF RIS model chains. (———, – – –) Interdependent RIS model with non-local interactions given by Sutherland potentials with $r_c = 0.27$ nm. (———) $c = 0$; (– – –) $c = -0.65$ J nm^6 mol^{-1}. (·····) Unperturbed interdependent RIS model ($\langle r^2_{0,\mathrm{int}}\rangle/n$). Values of T (K) given with curves

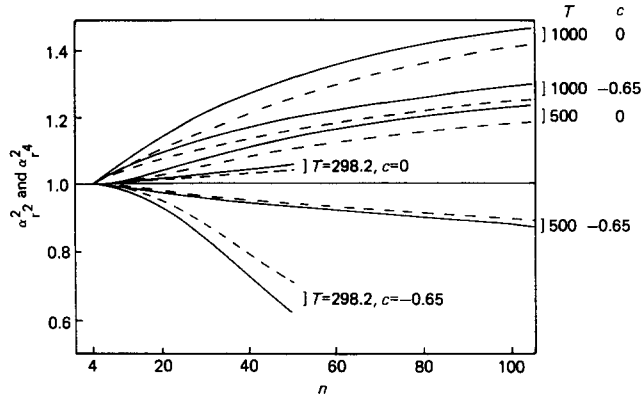

Figure 5 Expansion factors $\alpha^2_{r^2}$ and $\alpha^2_{r^4}$ on the bases of $\langle r^2_{0,int}\rangle$ and $\langle r^4_{0,\mathrm{int}}\rangle$, respectively, *versus* n. (———) $\alpha^2_{r^2}$; (– – –) $\alpha^2_{r^4}$. Non-local interactions and temperatures as *Figure 4*. Values of T (K) and c (J nm^6 mol^{-1}) given with curves

temperature. This is because $\langle r^2_{0,\mathrm{int}}\rangle$ decreases as temperature increases, giving more compact configurations having more segmental overlaps.

Variation of expansion factors with n *and* T

The perturbation theory of the freely-jointed chain leads to the following expression for the even moments of the end-to-end distance distribution[24,25]

$$\langle r^{2p}\rangle = \langle r_0^{2p}\rangle\left(1 + \sum_{m=1}^{p} \frac{(-1)^{m+1}}{(4m^2-1)} \times 4\left(\frac{p}{m}\right) z - \ldots\right), \quad (30)$$

where $p = 1, 2, \ldots$, and z is the usual excluded-volume parameter. Hence,

$$\alpha^2_{r^2} = \langle r^2\rangle/\langle r_0^2\rangle = 1 + (4/3)z - \ldots \quad (31)$$

and

$$\alpha^2_{r^4} = (\langle r^4\rangle/\langle r_0^4\rangle)^{1/2} = 1 + (6/5)z - \ldots \quad (32)$$

where, for present purposes, $\langle r_0^q\rangle$ is taken as $\langle r^q_{0,\mathrm{int}}\rangle$. Equations (31) and (32) suggest that for positive z (expansion), $\alpha^2_{r^2} > \alpha^2_{r^4}$, and for negative z (contraction), $\alpha^2_{r^2} < \alpha^2_{r^4}$. That is, higher moments, which are more characteristic of extended configurations, are less affected by segment–segment interactions, resulting in uneven expansion of the molecular coil. Such behaviour is found for the chains in *Figure 4*, as shown in *Figure 5*, where $\alpha^2_{r^2}$ and $\alpha^2_{r^4}$ are plotted as functions of n.

For more strongly attractive potentials, such as the L–J/CP potential, the behaviour

$$|\alpha^2_{r^4} - 1| < |\alpha^2_{r^2} - 1|, \quad (33)$$

does not hold at shorter chain lengths. In fact, the relative values of expansion coefficients of various moments shows subtle changes depending on the frequencies of possible separations of pairs of segments (r_{ij}) and the energies of such separations, as defined by the potential function used. Relative increases of statistical weights, compared with those of the unperturbed chain, of configurations with end-to-end distances less than $\langle r^4\rangle^{1/4}$ and $\langle r^2\rangle^{1/2}$ will decrease $\langle r^4\rangle$ and $\langle r^2\rangle$, respectively. The unperturbed chains have $\langle r_0^2\rangle^{1/2} < \langle r_0^4\rangle^{1/4}$, hence, a sufficient condition for the observed behaviour is that $E(r_{ij})$ decreases or increases monotonically to zero as r_{ij} increases. However, if the potential has a minimum, this condition will not be met for all r_{ij}. With a high proportion of separations r_{ij} less than that of the minimum of the potential function used, the overall effect can be that $\langle r^4\rangle^{1/2}$ is reduced by more than $\langle r^2\rangle$.

A general point to be noted from *Figure 5* is that the use of realistic unperturbed dimensions and the Sutherland form of potential allows both small and large excluded-volume effects to be modelled. Often, excluded volume effects in relatively short chains[17,23] are much larger than those observed experimentally. For example, diffusive behaviour [4,26,27] shows that excluded-volume effects are often negligible for chains of less than about 100 bonds.

Evaluation of effective cluster integrals

Two-parameter theories of excluded volume predict generally that the expansion coefficient (α_{r^2}) is a function of z which itself is a function of n and β.

That is

$$z = \left(\frac{3}{2\pi\langle r_0^2\rangle}\right)^{3/2} \beta n^2. \quad (34)$$

The theories use freely-jointed chains and are strictly valid only in the limit $n \to \infty$. Of the numerous theories, perturbation theory, valid as $z \to 0$, gives equation (31) for $\alpha^2_{r^2}$, whilst the Flory theory as modified by Stockmayer[28] gives

$$\alpha^5_{r^2} - \alpha^3_{r^2} = (4/3)z \quad (35)$$

Equation (35) agrees with perturbation theory as $z \to 0$ and gives proportionality between $\alpha^5_{r^2}$ and z as $z \to \infty$, as predicted by simple scaling arguments[29]. The values of β given by these two theories for the present chains are now examined through the calculated values of $\alpha^2_{r^2}$ as they represent extremes of the numerical values of α_{r^2} given by two-parameter theories. It is interesting to see whether β becomes constant over the range of chain lengths studied and to compare the values of β found with those characteristic of the potentials used, i.e. β_{calc} of equation (7).

To evaluate β according to a given theory, equation (34) is rearranged to give

$$\beta = z\left(\frac{3}{2\pi\langle r_0^2\rangle}\right)^{3/2}/n^2 \qquad (36)$$

with z evaluated from equation (31) or from equation (35) using the known value of α_{r^2}. Actual chains require an arbitrary definition of n because β and n do not occur independently in the expressions for α_{r^2}. Two definitions clearly suggest themselves for consideration:

(1) Use of the conventional freely-jointed chain of n' links of length b, based on $\langle r_0^2\rangle$ and r_{max}, with

$$\langle r_0^2\rangle = \langle r_{0,int}^2\rangle = n'b^2$$

and (37)

$$r_{max} = n'b$$

where $\langle r_{0,int}^2\rangle$ is that calculated on the basis of interdependent local interactions and r_{max} is the value for the all-*trans* chain. The resulting values of β are the effective values per equivalent freely-jointed segment and are denoted β_{eff}.

(2) Identification of $\langle r_0^2\rangle$ with $\langle r_{0,int}^2\rangle$ and of n with the actual number of chain bonds in the chain. This gives the effective value of β per CH_2 group and is denoted accordingly β_{CH_2}.

Since excluded-volume theories are based on freely-jointed chains, the first approach would seem to be more correct. However, β_{eff} for actual chains relates to different numbers of segments because the relation between n and n' varies with chain flexibility and chain length[1,18]. Comparisons with β_{calc} are also somewhat ambiguous. The second approach gives the effective value of β_{CH_2} which may be compared directly with β_{calc}.

Figure 6 shows β_{eff} *versus* n' at 1000, 500 and 298.2 K for $c = -0.65$ J nm^6 mol^{-1} determined using the first-order perturbation and modified Flory theories to evaluate z from α_{r^2}. At the higher temperatures, reasonably constant values of β_{eff} are obtained. For the highly contracted chains at 298.2 K, the tendency to a constant value is not apparent by 50 bonds. It was difficult to study longer, highly contracted chains because of the slowness of convergence.

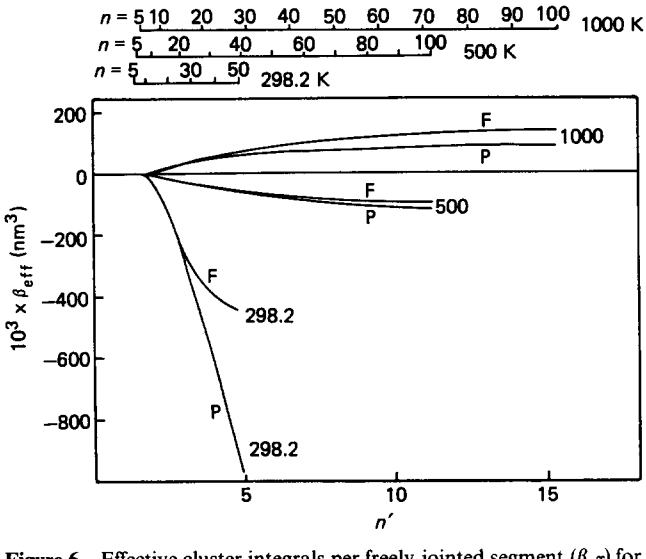

Figure 6 Effective cluster integrals per freely-jointed segment (β_{eff}) for the Sutherland potential with $c = -0.65$ J nm^6 mol^{-1} *versus* n', the number of freely-jointed links in a PM chain of n bonds. β_{eff} evaluated according to equations (36) and (37). (P) z evaluated according to first-order perturbation theory, equation (31). (F) z evaluated according to modified Flory theory, equation (35). Values of T (K) given with curves. Uppermost scales relate n and n' at the various temperatures used

Figures 7a and *7b* show the values of β_{CH_2} at 500 K and 1000 K using the first-order perturbation and modified Flory theories for the hard-core potential ($c = 0$) and the same Sutherland potential as in *Figure 6*. A tendency to constant values of β is again indicated. Notice that, although β_{calc} for $c = 0$ is independent of temperature, β_{CH_2} is not. This behaviour results from the temperature dependences of the statistics of the unperturbed chains. More *gauche* states occur at higher temperaures. Hence, smaller r_{ij} occur more frequently, more non-local exclusion occurs and β_{CH_2} increases.

It is apparent from *Figures 6* and *7* that two-parameter expressions can be used to model actual chains, provided the chain is sufficiently flexible and long, and contraction or expansion is not too marked. For PM, $n \sim 100$ is required at the (hypothetical) temperature of 1000 K and $c = -0.65$ J nm^6 mol^{-1}. Longer chain lengths are required for stiffer chains. Alternatively, β may be allowed to vary as a function of chain length, when shorter chain lengths may be used. The fact that $\langle r_0^2\rangle/n$ is constant is not a sufficient condition for a constant value of β. It is clear from *Figure 3* that $\langle r_{0,int}^2\rangle/n$ has almost reached its limiting values at $n \sim 100$ at 298.2, 500 and 1000 K.

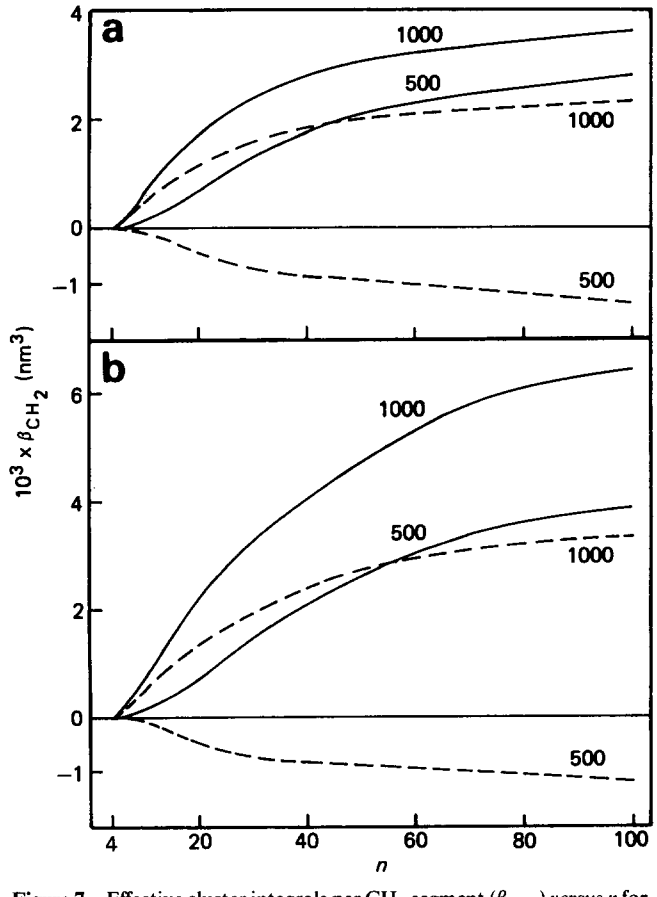

Figure 7 Effective cluster integrals per CH_2 segment (β_{CH_2}) *versus* n for the Sutherland potentials with $c = 0$ (———) and $c = -0.65$ J nm^6 mol^{-1} (– – –). Values of T (K) given with the curves. (a) z evaluated according to first-order perturbation theory. (b) z evaluated according to modified Flory theory

The values of β_{CH_2} given in *Figure 7* at the longer chain lengths are much smaller than β_{calc} for the potentials used. Values of β_{CH_2} for 80 and 100 bonds and of β_{calc} are shown in *Table 2*. β_{CH_2} is between one and two orders of magnitude smaller than β_{calc}. Regarding perturbation theory, the constant C in the generalized form of equation (31)

$$\alpha_{r^2}^2 = 1 + Cz - \ldots \quad (38)$$

only attains the value 4/3 at infinite chain length. For $n = 100$, C may be variously estimated to decrease to maybe half this value[30-32]. However, the resulting increase in β_{CH_2} by a factor of up to two still leaves it much smaller than β_{calc}.

Also shown in *Table 2* are values of β_{eff}/m, where m is the number of real bonds per freely-jointed link[18]. Thus, β_{eff}/m is the average excluded-volume contribution per bond on the basis of the equivalent freely-jointed chain for the particular chain length (n) and temperature. In all cases, β_{eff}/m is also smaller than β_{calc}. The smaller values of β_{CH_2} and β_{eff}/m compared with β_{calc} are primarily a result of the connectivity of segments. β_{calc}, equation (7), assumes that interacting pairs of segments have mutual separations from 0 to ∞. This is clearly not possible. The present calculations show that the effects of restricting segments are large. It is not possible, therefore, to model chain dimensions from *ab initio* calculations based on a given potential. The potential must be incorporated into the chain structure and local and non-local interactions evaluated together. They are not independent; the mutual configurational space accessible to a pair of segments i and j depends on r_{ij}. The probabilities of various r_{ij}'s are not only related to $|i-j|$ but also to the flexibility of the chain between i and j (and to the local and non-local interactions of all the other segment pairs).

The effects of local chain structure may be seen approximately by taking the ratio β_{eff}/m to β_{CH_2}, as in *Table 2*. At 500 K, β_{eff}/m is about nine times larger than β_{CH_2} and at 1000 K about six-and-a-half times larger. Thus, for PM at 500 K (or 1000 K) non-local interactions really contribute only about 1/9 (or 1/6.5) of the total excluded volume per CH_2 segment, calculated on the basis of the equivalent freely-jointed chains. The majority of the excluded volume is due to *trans–gauche* energy differences and valence-angle restrictions limiting the mutual space available to pairs of segments.

Table 2 Values of β_{CH_2}, β_{calc} and β_{eff}/m for PM chains of 80 and 100 bonds at 500 and 1000 K and Sutherland potentials with $r_c = 0.27$ nm and $c = 0$ and -0.65 J nm^6 mol^{-1}. β_{CH_2} and β_{eff}/m evaluated using first-order perturbation (P) and modified Flory (F) theories. $m = n/n'$ is the number of real bonds per freely-jointed link. Units of β are 10^{-3} nm^3 (= Å^3)

	500 K		1000 K	
n	80	100	80	100
	$c = 0$ J nm^6 mol^{-1}			
β_{CH_2} (P)	2.59	2.80	3.45	3.59
β_{CH_2} (F)	3.55	3.82	5.99	6.34
β_{calc}	82.45		82.45	
β_{eff}/m (P)	24.0	25.7	22.6	23.3
β_{eff}/m (F)	30.7	33.9	39.5	42.2
$(\beta_{eff}/m)/\beta_{CH_2}$ (P)	9.27	9.18	6.55	6.49
$(\beta_{eff}/m)/\beta_{CH_2}$ (F)	8.65	8.87	6.59	6.66
	$c = -0.65$ J nm^6 mol^{-1}			
β_{CH_2} (P)	−1.19	−1.38	2.21	2.27
β_{CH_2} (F)	−1.05	−1.20	3.14	3.30
β_{calc}	46.74		65.23	
β_{eff}/m (P)	−11.7	−12.9	13.3	13.7
β_{eff}/m (F)	−9.78	−10.6	20.9	21.4
$(\beta_{eff}/m)/\beta_{CH_2}$ (P)	9.83	9.34	6.02	6.04
$(\beta_{eff}/m)/\beta_{CH_2}$ (F)	9.31	8.83	6.66	6.48

The preceding comparisons of the values of β_{calc}, β_{CH_2} and β_{eff}/m in *Table 2* and the plots in *Figures 6* and *7* show clearly that, whilst two-parameter theories may give reasonable functional forms for the dependence of α_{r^2} on z, the effective value of the excluded volume per segment cannot be derived directly from the segment–segment potential function. Similar observations have been made by Yamakawa[33] on the basis of the comparison of experimental values of second virial coefficients and intramolecular expansion factors.

Effective generalized θ-points

The θ-point is usually defined as the temperature at which $\langle r^2 \rangle$ attains its unperturbed value, $\langle r_{0,int}^2 \rangle$, in the limit if infinite chain length. Also, $\langle s^2 \rangle$ is usually assumed to have its unperturbed value, $\langle s_{0,int}^2 \rangle$ at the same temperature. However, a single θ-point at which all moments of the distributions in r and s assume their unperturbed values appears to be inconsistent with the uneven expansion of the molecular coil, e.g. in *Figure 5*, $|\alpha_{r^4}^2 - 1| < |\alpha_{r^2}^2 - 1|$, inequality (33). By calculating $\langle r^q \rangle$ and $\langle r_{0,int}^q \rangle$, $q = 1, 2, \ldots, 10$ at various temperatures it was possible to find graphically those θ-temperatures, θ_{r^q}, at which $\langle r^q \rangle = \langle r_{0,int}^q \rangle$. *Figures 8a–d* show the results for four Sutherland potentials as a function of $1/n$. There are uncertainties in the extrapolated values of θ_{r^q} at $1/n = 0$ because, due to lack of computer time, the maximum value of n used was only 20 or 30. However, the results indicate ranges of θ-temperatures at infinite chain length, characteristic of the various moments and potential functions, as summarized in *Table 3*. The ranges of 10–20 K are probably too small to be detected experimentally, hence validating the experimental concept of a single, average θ-temperature, which will in fact vary with the property (or moment of the spatial segmental distribution) being measured.

All the potentials give θ_{r^q} increasing as q increases, i.e. $\theta_r < \theta_{r^2} < \ldots \theta_{r^{10}}$, with the θ-temperatures drawing closer together at the larger values of q. This behaviour is characteristic of uneven expansion, with configurations of longer end-to-end distances being less perturbed than those of shorter ones (cf. *Figure 5*). The decrease in the range of θ-temperatures as chain length increases arises from the fractions of excluded configurations (those with one or more intersegmental separations r_{ij} falling within the repulsive core of the potential) becoming smaller, and the statistical weights of the remaining configurations becoming more insensitive to the potential function as longer segmental separations become more significant. Thus, $E_{non\text{-}local}$ per bond becomes smaller. However, only in the hypothetical limit of $E_{non\text{-}local} = 0$ for all configurations will a unique θ-point result, independent of moment.

It can be seen that the form of the variation of θ_{r^q} with $1/n$ depends on the potential function. The most attractive potential, *Figure 8d*, gives θ-temperatures

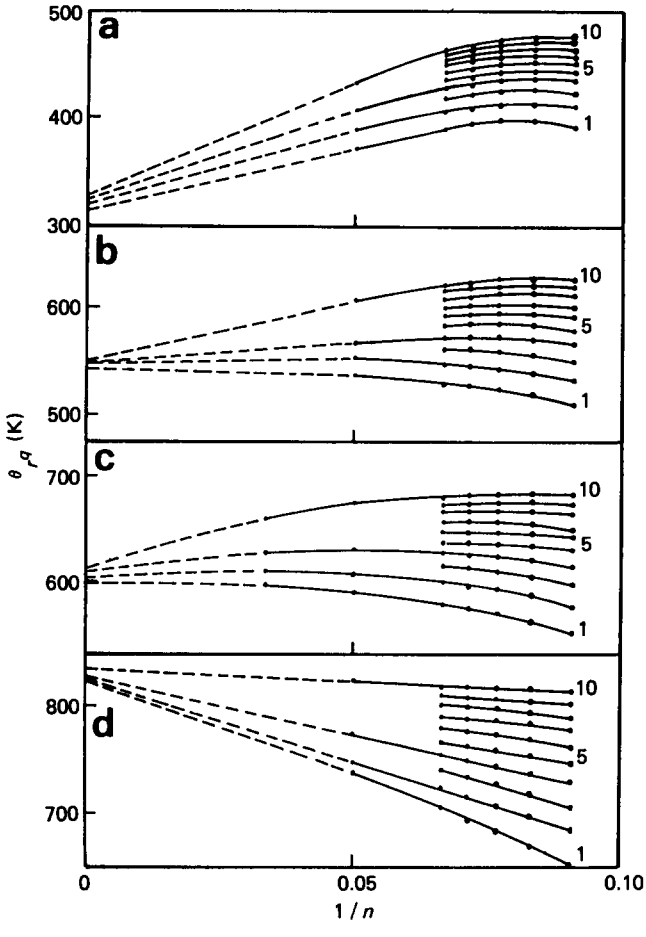

Figure 8 θ-temperatures (θ_{r^q}) on the bases of various moments ($\langle r^q \rangle$) *versus* $1/n$. $q = 1, 2, \ldots, 10$; values of $q = 1$, 5, 10 indicated with curves. Sutherland potentials used: (a) $c = -0.2337$ J nm^6 mol^{-1}; (b) $c = -0.5236$ J nm^6 mol^{-1}; (d) $c = -0.9726$ J nm^6 mol^{-1}

Table 3 Limiting ranges of θ-temperatures and ratios c/RT for Sutherland potentials with $r_c = 0.27$ nm and various values of c

c (J nm^6 mol^{-1})	Range of θ_{r^q} (K)	Range of 10^4 (c/RT)
−0.2337	314 to 327	−0.86 to −0.90
−0.5236	543 to 552	−1.14 to −1.16
−0.6500	598 to 612	−1.28 to −1.31
−0.9726	825 to 835	−1.40 to −1.42

which increase with chain length. The least attractive, *Figure 8a* shows maxima between 10 and 20 bonds, and then θ-temperatures which decrease as chain length increases. To explain the variations in shape, it should be remembered that expansion occurs because of the exclusion of configurations with small r_{ij}'s due to the hard core. Above θ, such expansion is partially counteracted by the effects of the attractive part of the potential, which, because $E(r)$ *increases* to zero as $r \rightarrow \infty$, statistically contracts the remaining configurations. As the temperature is lowered, the configurations with the smaller r_{ij}'s, those lying in the more attractive parts of the potential, are emphasized relative to configurations with larger r_{ij}'s. Thus, an increase in θ_{r^q} with n means that the hard-core exclusion of contracted configurations becomes less important relative to the statistical contraction of the remaining configurations due to the attractive well. This occurs when the well is sufficiently deep and broad, as in *Figure 8d*. A decrease in θ_{r^q} with increasing n means that the non-excluded configurations become statistically less contracted as n increases so that lower temperatures are required to emphasize the more contracted configurations. Such behaviour occurs most with the weakest potential (*Figure 8a*), for the larger values of n and particularly for the higher moments (also in *Figures 8b* and *8c*), which emphasize the configurations with larger r_{ij}'s. The increase in θ_{r^q} with n for the smaller values of n and the weakest potential arise because of the smaller values of r_{ij}, which are influenced more by the potential well. Conventional polymer theories[29,34] consider only θ_{r^2} and predict an increase with n, as in *Figure 8d*.

Returning to *Table 3*, it can be seen that the θ-points for infinite chain length increase with the atrractiveness of the potential, as denoted by a larger negative value of c. For a freely-jointed or freely-rotating chain in which all unperturbed configurations have $E_{\text{local}} = 0$; the value of c/RT at the θ-points assumes a value independent of c for a given value of r_c. This arises from the fact that any change in c multiplies $E_{\text{non-local}} (= c\Sigma r_{ij}^{-6})/RT$ by the same factor. *Table 3* shows that the magnitude c/RT at the θ-points increases as c decreases, i.e. the potential becomes more attractive. $|c/RT|$ can be considered as a measure of the attraction required to restore a chain to its unperturbed value. Thus, the weaker potentials, with lower θ-points and hence, more rigid (unperturbed) chains, require less attraction. For the hypothetical chain of disconnected segments, c/RT at the θ-point would be equal to that value required to make $\beta_{\text{calc}} = 0$. For Sutherland potentials with $r_c = 0.27$ nm, the value of c/RT is -3.32×10^{-4} nm^6. The larger value of $|c/RT|$ compared with those from *Table 3* again reflects the effects of chain structure on restricting segment–segment configurational space and interactions.

Comparison with results from lattice chains

The importance of accounting correctly for chain structure when considering effects of excluded volume is apparent from the previous sections. It may be illustrated further by investigating whether equivalent lattice chains can be used to give properties which scale to those of actual chains. Tetrahedral lattices give a reasonable approximation to the rotational states of the carbon back-bone. However, second-neighbour interactions are required to account for the $g_{\pm}g_{\mp}$ interaction. Results using such interactions are not presently available. Hence, the results of Clark and Lal[23], using a tetrahedral lattice with a $g_{\pm}$ energy of $1kT$ and no additional $g_{\pm}g_{\mp}$ energy, are considered instead.

In the work of Clark and Lal, simulation of change of solvent was effected by varying the nearest-neighbour interaction parameter, ΔE_s, denoting the energy change when a site next to a segment becomes full (i.e. becomes occupied by another segment). ΔE_s is defined by the quasi-chemical equilibrium equation

$$\Delta E_s = E_{11} + E_{22} - 2E_{12} \qquad (39)$$

where E_{11} is the energy when two neighbouring sites are empty (solvent–solvent pair), E_{22} the energy when they are occupied by segments (segment–segment pair) and E_{12} is the energy of an empty-occupied (solvent–segment) pair. Comparison with equation (1) shows that

$-\Delta E_s = 2\Delta E_{12}$. Further, the Flory parameter, χ, is defined as

$$\chi = z'\Delta E_{12}/kT = -(z'/2)\Delta E_s/kT \qquad (40)$$

where z' is the effective lattice coordination number for segment–solvent contacts involving the internal segments of a chain (i.e. chain-ends are neglected). Clark and Lal used values of $\Delta E_s/kT$ between 0.5 and -1.5 to reflect changes of solvent quality. Their results for a 50-bond chain are plotted in *Figure 9*, as $\alpha^2_{r^2,\mathrm{ind}}$ *versus* $\Delta E_s/kT$, with $\alpha^2_{r^2,\mathrm{ind}} = \langle r^2\rangle/\langle r^2_{0,\mathrm{ind}}\rangle$, taking for $\langle r^2_{0,\mathrm{ind}}\rangle$ the values appropriate to the particular lattice used. The θ_{r^2}-point occurs at $\Delta E_s = -0.36kT$.

With off-lattice chains, the parameter β takes the place of χ. The two parameters are related formally for an infinite chain by the equation

$$\beta = 2v_1(1/2 - \chi) \qquad (41)$$

where v_1 is the molecular volume of the solvent. In terms of ΔE_s, one has, from equation (40),

$$\beta = v_1(1 + z'(\Delta E_s/kT)) \qquad (42)$$

This equation provides the basis for correlating results for lattice and off-lattice chains. However, the parameters are not known independently. For off-lattice chains, β is formally β_{calc}, but as previously discussed, the effective value per segment ($\beta_{\mathrm{CH_2}}$) is a much smaller quantity and can only be determined *a posteriori*. For lattice chains, z' is the effective lattice coordination-number because segment occupation is not random. Accordingly, v_1 is also not known. A fixed point at which equation (42) is satisfied must be decided upon and then z' can be chosen to convert a scale in $\Delta E_s/kT$ to one in β_{calc}. In addition, for off-lattice chains, β_{calc} can be varied by changing the potential or the temperature. For the present analysis, the temperature was fixed at 298.2 K, corresponding approximately to the $g_\pm$ energy of $1kT$ used by Clark and Lal, and β_{calc} was varied by using the potentials listed in *Table 1*.

The present off-lattice results for 50 bonds are shown as the solid curve in *Figure 10*, *with* $\alpha^2_{r^2,\mathrm{int}}$ plotted *versus* β_{calc}. The lattice results from *Figure 9* have been matched at the

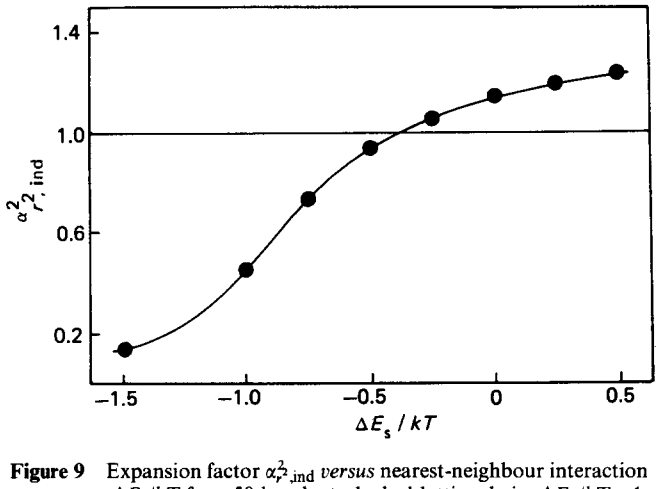

Figure 9 Expansion factor $\alpha^2_{r^2,\mathrm{ind}}$ *versus* nearest-neighbour interaction parameter, $\Delta E_s/kT$, for a 50-bond tetrahedral-lattice chain; $\Delta E_\sigma/kT = 1$, $\Delta E_\omega/kT = 0$. Derived from results of Clark and Lal[23]

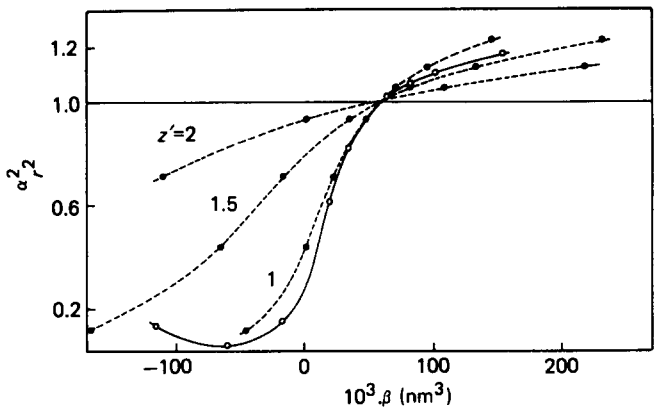

Figure 10 Expansion factors $\alpha^2_{r^2}$ for 50-bond interdependent RIS off-lattice chains and tetrahedral lattice chains. (———) Off-lattice chains: $\beta = \beta_{\mathrm{calc}}$ at 298.2 K (see *Figure 1*); $\alpha^2_{r^2} = \alpha^2_{r^2,\mathrm{int}}$. (– – –) Lattice chains: as *Figure 9* for values of z' given with curves using $\Delta E_s/kT$ ($= -0.36$) matched with β_{calc} ($= 61 \times 10^{-3}$ nm^3) at the θ_{r^2}-point (equation (43)) and then β calculated according to equation (42)

θ-point, $\Delta E_s/kT = -0.36$, giving an equivalent value of β equal to 61×10^{-3} nm^3. Other equivalent values of β at various $\Delta E_s/kT$ for chosen z' may then be calculated from equation (42), after using the condition

$$61 = v_1(1 - 0.36z') \qquad (43)$$

to define v_1. Curves (dashed) corresponding to $z' = 1$, 1.5 and 2 are shown in *Figure 10*. It is known that non-random occupation decreases z' below its random value of 2. However, no single value of z' allows the lattice results to scale to the off-lattice results. *Figure 10* emphasises again the importance of accounting properly for local interactions when modelling chain behaviour. The lattice used by Clark and Lal was more elaborate then others often used in lattice calculations, for which larger variations in z' would be expected. The situation may be improved if second-neighbour ($g_\pm g_\mp$) interactions are introduced, but then much of the simplicity of the lattice calculations is lost.

SUMMARY AND CONCLUSIONS

The development of an algorithm reducing rounding errors when moving parts of chains in external space means that realistic rather than lattice or freely-jointed chains can be used in Monte–Carlo calculations involving perturbed chains. The present calculations involving the PM chain show that chain structure is important and must be properly accounted for before meaningful expansion factors can be evaluated. The modelling of real chains at actual temperatures then becomes possible.

The Sutherland potential is seen to be a useful potential function, allowing systematic variation of its parameters. Given the usual approximation of a solvent continuum, the use of Sutherland functions and realistic chain models is recommended for modelling actual chain behaviour. Chain structure influences greatly the effective value of the segment–segment cluster integral, $\beta_{\mathrm{CH_2}}$ or β_{eff}/m. The integral cannot be predicted *ab initio* from the potential function used. Further, the simple scaling of lattice chains to reproduce properties of actual chains is not possible.

The uneven expansion of chains means that the concept of a single θ-point is not strictly valid. The present evaluations of θ_{r^2} need to be extended to longer chains

and to other chain structures to ascertain whether θ-ranges at infinite chain length are experimentally significant. The present calculations were carried out using a CDC 7600. Array processors and the vectorization of algorithms will enable longer chain lengths to be studied.

ACKNOWLEDGEMENTS

One of us (D.R.) gratefully acknowledges the receipt of an SERC Studentship and an SERC Research Assistantship during the period of this work.

REFERENCES

1 Flory, P. J. 'Statistical Mechanics of Chain Molecules', Interscience, Publishers, London, 1969
2 Abe, A., Jernigan, R. L. and Flory, P. J. *J. Am. Chem. Soc.* 1966, **88**, 631
3 Mokrys, I. J., Rigby, D. and Stepto, R. F. T. *Ber. Bunsenges. Phys. Chem.* 1979, **83**, 446
4 Edwards, C. J. C., Rigby, D. and Stepto, R. F. T. *Macromolecules* 1981, **14**, 1808
5 Edwards, C. J. C., Kaye, A. and Stepto, R. F. T. *Macromolecules* 1984, **17**, 773
6 Edwards, C. J. C. and Stepto, R. F. T. in 'Physical Optics of Dynamic Phenomena and Processes in Macromolecular Systems', Ed. B. Sedlaček, Walter de Gruyter and Co., Berlin, 1985, p. 1
7 Dodgson, K., Edwards, C. J. C. and Stepto, R. F. T. *Br. Polym. J.* 1985, **17**, 14
8 Winnick, M. A., Rigby, D., Stepto, R. F. T. and Lemaire, B. *Macromolecules* 1980, **13**, 699
9 Rigby, D. and Stepto, R. F. T. *Faraday Disc. Chem. Soc.* 1979, **68**, 443
10 Lal, M. and Stepto, R. F. T. *J. Polym. Sci., Polym. Symp. Edn.* 1977, **61**, 401
11 Higuchi, A., Rigby, D. and Stepto, R. F. T. in 'Adsorption in Solution' (Eds. R. H. Ottewill, C. H. Rochester and A. L. Smith), Academic Press, London, 1983, p. 273
12 Edwards, C. J. C., Rigby, D., Stepto, R. F. T., Dodgson, K. and Semlyen, J. A. *Polymer* 1983, **24**, 391
13 Edwards, C. J. C., Rigby, D., Stepto, R. F. T. and Semlyen, J. A. *Polymer* 1983, **24**, 395
14 Edwards, C. J. C., Richards, R. W., Stepto, R. F. T., Dodgson, K., Higgins, J. S. and Semlyen, J. A. *Polymer* 1984, **25**, 365
15 Edwards, C. J. C., Richards, R. W. and Stepto, R. F. T. *Macromolecules* 1984, **17**, 2147
16 Edwards, C. J. C., Richards, R. W. and Stepto, R. F. T. *Polymer* 1986, **27**, 643
17 Lal, M. and Spencer, D. *Mol. Phys.* 1971, **22**, 649
18 Hill, J. L. and Stepto, R. F. T. *Trans. Faraday Soc.* 1971, **67**, 3202
19 Clark, A. T. and Lal, M. *Disc. Faraday Soc.* 1978, **65**, 227
20 Appleyard, A., Rigby, D. and Stepto, R. F. T. Proc. IUPAC 26th International Symposium on Macromolecules, Mainz, 1979, Vol. II, p. 723
21 Margenau, H. and Murphy, G. M. 'The Mathematics of Physics and Chemistry', van Nostrand, New York, 1946, Ch. 9, Section 5
22 Maxwell, E. A. 'Coordinate Geometry with Vectors and Tensors', Oxford University Press, 1958, Ch. 2, Section 14
23 Clark, A. T. and Lal, M. *Br. Polym. J.* 1977, **9**, 92
24 Yamakawa, H. and Kurata, M. *J. Phys. Soc. Jpn.* 1958, **13**, 78
25 Kurata, M., Yamakawa, H. and Teramoto, E. *J. Chem. Phys.* 1958, **28**, 785
26 Couper, A. and Stepto, R. F. T. *Trans. Faraday Soc.* 1969, **65**, 2486
27 Edwards, C. J. C., Stepto, R. F. T. and Semylen, J. A. *Polymer* 1980, **21**, 781
28 Stockmayer, W. H. *Macromol. Chem.* 1960, **35**, 54
29 de Gennes, P. G. 'Scaling Concepts in Polymer Physics', Cornell University Press, Ithaca, New York, 1979
30 Yamakawa, H. *J. Chem. Phys.* 1966, **45**, 2606
31 Bruns, W. *J. Chem. Phys.* 1980, **73**, 1970
32 Rigby, D. *Ph.D. Thesis*, University of Manchester, 1981
33 Yamakawa, H. *J. Chem. Phys.* 1973, **58**, 1523
34 Flory, P. J. 'Principles of Polymer Chemistry', Cornell University Press, Ithaca, New York, 1953